Calibration and Performance Evaluation of Omnidirectional Sensor with Compound Spherical Mirrors

Yuichiro KOJIMA Ryusuke SAGAWA Tomio ECHIGO Yasushi YAGI

The Institute of Scientific and Industrial Research, Osaka University
8-1 Mihogaoka, Ibaraki, Osaka, 567-0047, JAPAN
Email: {y-kojima, sagawa, echigo, yagi}@am.sanken.osaka-u.ac.jp

Abstract

We have proposed a correspondenceless stereo system that consists of a single camera with multiple omnidirectional mirrors, which can detect approaching close objects without finding correspondences along epipolar lines. The system offers omnidirectional observation, portability, and real-time detection of near objects. The detection method requires for creating a model of the shape and location of the mirrors. However, it is difficult to make the model accurately because small positioning errors for mirrors enlarge erroneous detection of near objects. This paper describes a method for calibrating a multiple omnidirectional mirror sensor through observing a point light source at an infinite range. It also evaluates detectable distances at every pixel by analyzing in simulated experiments. As a result, it is proved that the detectable distance is enhanced by using a combination of various mirrors and that it is in proportion to the resolution of the image and the size of mirrors.

1 Introduction

Recently, many surveillance cameras have been placed in street environments for crime prevention. However, crimes are committed more in places having a deserted feeling. In such places, a wearable security system is more effective than a fixed one. If a fixed security system is used, many cameras are necessary even though few people pass by; making this not a very efficient solution. On the other hand, since a wearable security system is individual equipment for each person, it can work anywhere. A wearable security system needs omnidirectional observation, portability, and real-time detection of near objects shown in Fig.1.

Several omnidirectional stereo systems have already been proposed. Two panoramic images acquired by rotating a camera are used for an omnidirectional stereo[3, 4]. But it is not suitable for detecting objects in real-time, since it is necessary to acquire images at a time. As another method, catadioptric stereo methods with two cameras [5, 7] use a parabolic and a hyperbolic mirror for each camera to generate an omnidirectional image. But two cameras are too large for this purpose, because a sensor fastened to a person needs to be small and light.

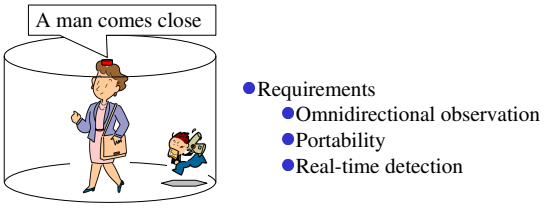

Figure 1: Wearable security system

We have proposed a correspondenceless stereo system that consists of a single camera with multiple omnidirectional mirrors, which can detect approaching close objects without finding correspondences along epipolar lines [1, 2]. The requirements of the system are omnidirectional observation, portability, and real-time detection of near objects. When an object is close enough to the sensor, the projected points of the object are different from corresponding points on the multiple omnidirectional mirrors. Meanwhile, when it is far from the sensor, its projected points are coincident at the corresponding points. The proposed method therefore detects near objects from differentiation between images of the multiple omnidirectional mirrors. For real-time detection, the proposed method computes corresponding points projected an object at an infinite range as preprocessing, which are saved as lookup table. Therefore, the system can detect objects in real-time without searching for corresponding points along epipolar lines.

The method detect objects by using a lookup table of points projected an object at an infinite range. When creating the table, the detection method requires for creating a model of the shape and location of the mirrors. However, as accurate information is difficult to obtain, it is difficult

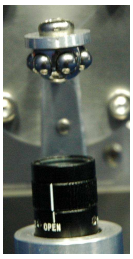

Figure 2: Omnidirectional camera with compound spherical mirrors

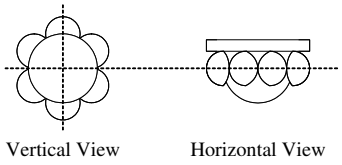

Figure 3: Configuration of compound spherical mirrors

Figure 4: An example of an image of the sensor.

to create the table without calibrating the system. This paper describes a method for calibrating a multiple omnidirectional mirror sensor through observing a point light source at an infinite range. Further, this method can use mirrors of any shapes.

Another issue is to find the best mirror shape for the system. We discussed the arrangement of paraboloidal mirrors in [2], and in this paper we analyze detectable distances of the system with the mirrors of arbitrary shape. However, the multiple mirrors constituting the system make it difficult to theoretically calculate detectable distances. Thus, we evaluate distances that have sufficient disparity as detectable distances at every pixel. As a result, we obtain how the detectable distance changes when the size or the arrangement of each mirror is changed. Since the applicable sizes and arrangements of the mirrors are evaluated, it is useful for improving performance.

2 Omnidirectional Sensor with Compound Spherical Mirrors

Our omnidirectional sensor consists of compound spherical mirrors. Fig.2 shows an experimental setup of the camera. The sensor has a large mirror and 6 small ones as shown in Fig.3.

Rays from an object hit these mirrors and reflected rays are projected on the image plane. Fig.4 shows an example of an image of the sensor. Because the centers of the side mirrors are not on the camera axis, the images on the side mirror are distorted. The rays that hit different mirrors intersect each other at the object position; thus, we can compute the range of the object by triangulation. However, since the length of the baseline is the distance of the points where the rays hit the mirrors, the baseline is quite narrow. As it is difficult to compute the range of objects at an arbitrary range, our method only determines if an object is at infinite range or not. This approach is applicable for a narrow baseline system and the computational cost is low.

3 Detection of Near Objects by Catadioptric Stereo

3.1 Computing Corresponding Points for an Infinite Range

In this section, we compute the corresponding points when an object at an infinite range is found in several of the sensor mirrors.

Fig.5 shows the situation for the central mirror. O is the origin of the camera coordinate system. d is the distance from the camera origin to the center of the mirror C, the radius of which is R. When an object is projected onto the point $\boldsymbol{x}$ in the central mirror, a ray from the object hits the mirror at the point $\boldsymbol{p}$, $\angle \boldsymbol{p}CO = \theta$, and $\angle \boldsymbol{p}OC = \phi$. And $\boldsymbol{x}$ is defined by using γ,

$$(c_x + l\cos\gamma, c_y + l\sin\gamma) \tag{1}$$

in the image coordinate system, where (c_x, c_y) is the image center. Then,

$$\tan\phi = \frac{l}{f} \tag{2}$$

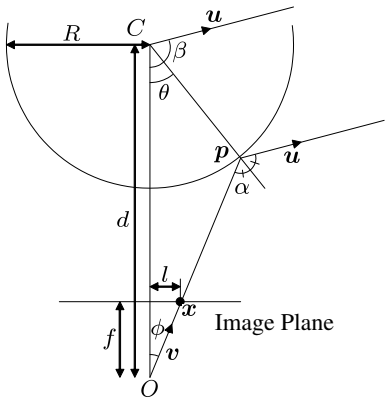

Figure 5: The ray direction reflected on the center mirror.

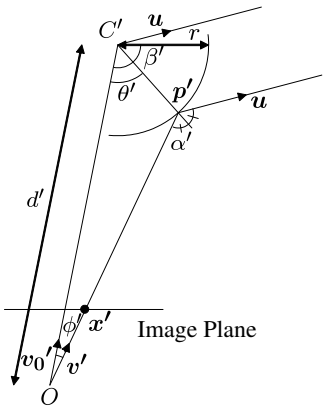

Figure 6: The ray direction reflected on one of the side mirrors.

where f(in pixels) is the focal length of the camera. By considering the triangle $\triangle \boldsymbol{p}CO$,

$$\tan\phi = \frac{R\sin\theta}{d - R\cos\theta}. \tag{3}$$

We compute θ by solving (3).

The incident angle α is $\theta + \phi$, because the normal vector at $\boldsymbol{p}$ is $\vec{C\boldsymbol{p}}$. Since the incident and reflected angles are the same,

$$\beta = \alpha + \theta = 2\theta + \phi. \tag{4}$$

Thus, the ray vector $\boldsymbol{u}$ from the mirror to the object becomes

$$(\cos\gamma\sin\beta, \sin\gamma\sin\beta, -\cos\beta). \tag{5}$$

If the object is at an infinite range, the ray directions from the object to the mirrors are parallel. Fig.6 shows a situation in which the same object is found in one of the side mirrors. The incident ray vector is parallel to $\boldsymbol{u}$. Since the unit vector $\boldsymbol{v}_0'$ from the origin O to the center of the side mirror C' is known,

$$\cos\beta' = -\boldsymbol{u}\cdot\boldsymbol{v}_0'. \tag{6}$$

In a manner similar to the case of the center mirror, we compute θ' by solving

$$\tan\phi' = \frac{r\sin\theta'}{d' - r\cos\theta'}, \tag{7}$$

where $\phi' = \beta' - 2\theta'$ and $d' = \sqrt{d^2 + R^2}$.

If the unit vector $\boldsymbol{w}$ is perpendicular to $\boldsymbol{v}_0'$ and $\boldsymbol{u}$, $\boldsymbol{w}$ is given by normalizing $\boldsymbol{v}_0' \times \boldsymbol{u}$. Then, the vector $\boldsymbol{v}' = (v_x', v_y', v_z')$ from the origin to the point $\boldsymbol{p}'$, where the ray hits the side mirror, is computed by rotating $\boldsymbol{v}_0'$ around $\boldsymbol{w}$ by angle ϕ'. Finally, the point $\boldsymbol{x}'$ on which the object is projected onto in the side mirror is computed as

$$(c_x + l'\cos\gamma', c_y + l'\sin\gamma'), \tag{8}$$

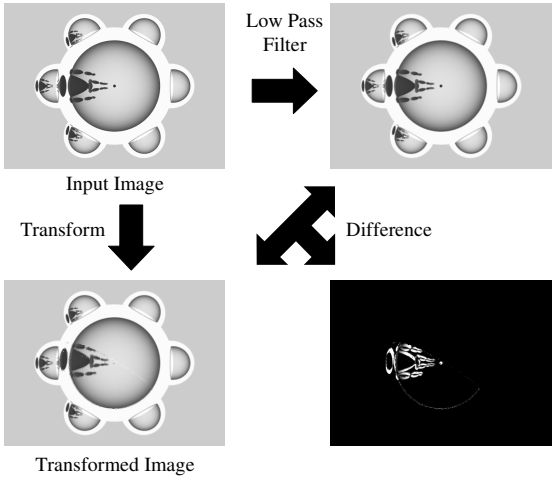

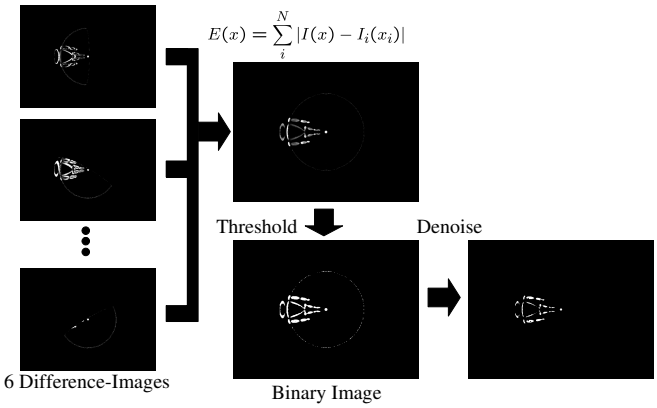

Figure 7: Flowchart of detecting near objects

where

$$l' = f\frac{\sqrt{v_x'^2 + v_y'^2}}{v_z'}, \tan\gamma' = \frac{v_y'}{v_x'} \tag{9}$$

Since the points are computed as preprocessing and these are saved as lookup table. When our method computes the difference between the images of the mirrors, it refers to a lookup table.

3.2 Detecting Near Objects

If an object is close enough to the sensor, the projected point of the object is different from the that of the object at an infinite range. Thus, our method takes into account the difference of the intensity between the images of the mirrors. The intensity of the central mirror is $I(\boldsymbol{x})$, and the intensity of the side mirror i is $I_i(\boldsymbol{x}')$. The criterion $E(\boldsymbol{x})$ to detect near objects becomes

$$E(\boldsymbol{x}) = \sum_i^N |I(\boldsymbol{x}) - I_i(\boldsymbol{x}')|, \tag{10}$$

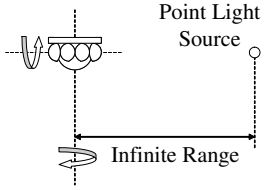

Figure 8: The calibration system that the sensor attached on turntables

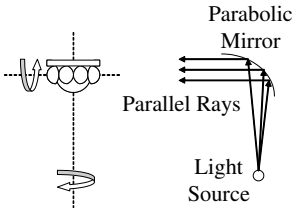

Figure 9: The calibration system using parabolic mirrors for making parallel rays

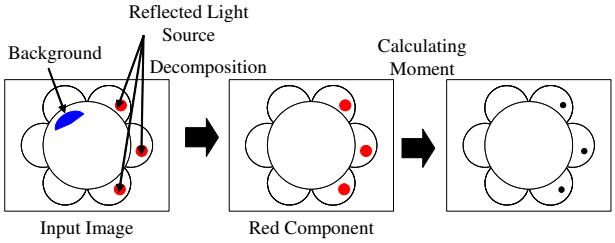

Figure 10: Flowchart for detecting corresponding points

where N is the number of side mirrors on which the object is projected onto.

The flowchart of actual processing is like Fig.7. This scene is generated by the ray tracing method. In this example, a person stands near the sensor. The image of a side mirror is transformed by projecting every point of the side mirror to the center image according to the correspondences. The near object is detected by taking into account the difference between the original center image and the transformed image. Since we obtain 6 difference images, we can use the sum of them. After removing the noise of the sum of the differences of images by erosion and dilation, the person standing near the sensor is detected.

4 Detecting Corresponding points for Calibration

For detecting near objects, the proposed method needs a lookup table of corresponding points for an infinite range. When creating the table, we need information about the shape of the mirrors and the locations of the camera and mirrors. However, as accurate information is difficult to obtain, it is also difficult to create the table and accurately calibrate the system.

We propose a method for detecting corresponding points through observing a point light source at an infinite range. This method can use the compound spherical mirrors, but it can also use mirrors of any shape. Since the light source is at an infinite range, the light is considered as a parallel one. By attaching the sensor on two turntables, the light source is observed while rotating the sensor as shown in Fig.8. The light is observed at several points in an image because the light is reflected by each mirror. We regard them as the corresponding points. The lookup table is obtained by finding these corresponding points while rotating the sensor. Fig.9 shows the system using parabolic mirror and light source instead of point light source at infinite range. Fig.10 shows the flowchart for detecting corresponding points from an image. For simplicity, we used a red light source and a blue background. After taking out the red component for removing the background image, the corresponding points become the centers of gravity of the light source in the image.

5 Estimation of Detectable Distance

Another issue is to find the best mirror shape for the system. In this section, we analyze the detectable distances of the system with the mirrors of arbitrary shape.

5.1 Simulation of Omnidirectional Sensor

In the previous section, we used compound spherical mirrors for the sensor. If a mirror of another shape is used, the detectable distance will change. For example, Fig.11 shows two examples, a large mirror and 8 small mirrors, and a large parabolic mirror and 6 small parabolic ones.

To evaluate the performance of a sensor with these mirrors, it is necessary to theoretically or experimentally compute the detectable distances of the sensor.

5.2 Calculating of Detectable Distance

Because detectable distances are different according to the position of the image, we calculate them for each pixel.

The corresponding points can be calculated by the equations described in Section 3.1. Fig.12 shows the ray direction reflected on the compound spherical mirrors. The ray from an infinite range is projected on the point $\boldsymbol{x}$ reflected

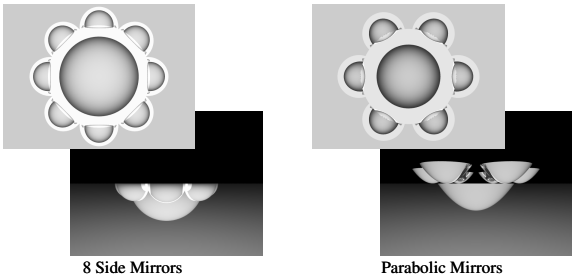

Figure 11: Examples of mirror shape for the sensor

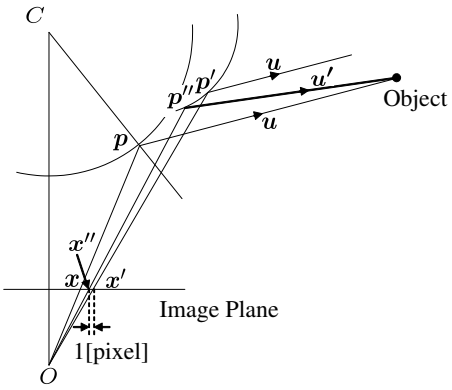

Figure 12: Ray direction when the sensor detects objects

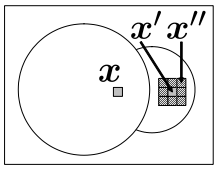

Figure 13: Location of the projected points on the image

by the center mirror, and then projected on the point $\boldsymbol{x}'$ reflected by the side mirror. Then, $\boldsymbol{x}$ and $\boldsymbol{x}'$ are corresponding points. If the sensor can detect objects, which are sufficiently near, the ray from the objects reflected on the side mirror is projected on the point $\boldsymbol{x}''$. $\boldsymbol{x}''$ is a point away from $\boldsymbol{x}'$ by 1 pixel. Therefore, the object exists at the intersecting point of the ray projected onto $\boldsymbol{x}$ and the one projected onto $\boldsymbol{x}''$. The detectable distance on $\boldsymbol{x}$ becomes the distance from C to the object.

However, even if all parameters are known, including those of the camera, mirrors and corresponding points, computing the intersecting point is still difficult if we use mirrors of intricate shapes. Therefore, we find an approximation of $\boldsymbol{x}''$ experimentally instead of computing the exact intersecting point. Now, we assume that $\boldsymbol{x}$, $\boldsymbol{x}'$ and $\boldsymbol{x}''$ take discrete positions on the image. On the assumption, as shown in Fig.13, $\boldsymbol{x}''$ is a point 1 pixel from $\boldsymbol{x}'$.

If an object exists at the point $\boldsymbol{X}$, which is the intersecting point of the ray reflected $\boldsymbol{p}$ on a mirror and the ray reflected $\boldsymbol{p}'$ on another mirror. Since $\boldsymbol{x}$ and $\boldsymbol{x}'$ are calculated discretely, the rays may not intersect. Thus, it is assumed that the object exists at a midpoint where these rays approach closest. Using independent parameters t_1 and t_2, the equations of these rays become as follows:

$$\begin{cases} \boldsymbol{X_1} = \boldsymbol{u}t_1 + \boldsymbol{p} \\ \boldsymbol{X_2} = \boldsymbol{u}'t_2 + \boldsymbol{p}'' \end{cases} \tag{11}$$

Since $\boldsymbol{X}$ is average of $\boldsymbol{X_1}$ and $\boldsymbol{X_2}$, $\boldsymbol{X}$ becomes

$$\boldsymbol{X} = \frac{\boldsymbol{X_1} + \boldsymbol{X_2}}{2} \tag{12}$$

where

$$f(t_1, t_2) = |\boldsymbol{X_1} - \boldsymbol{X_2}| \tag{13}$$

is minimized. We compute the distance of C to $\boldsymbol{X}$ for all neighboring pixels $\boldsymbol{x}''$ and choose one of $\boldsymbol{x}''$ that has the minimum distance between X_1 and X_2. The detectable distance is the distance of C to $\boldsymbol{X}$, which is computed by using the chosen $\boldsymbol{x}''$.

6 Experiments

6.1 Experiment of Detecting Corresponding Points

We experimented by detecting corresponding points of the sensor. The calibration system is shown in Fig.14. It consists of two turntables, with a sensor attached to each of them. The sensor is independently rotated in the directions of two axes. Since a ray from a point light source at an infinite range is a parallel ray, we use a parallel ray instead of a point light source at an infinite range. Each turntable is rotated 360 degree, and at every one degree images are taken. We take out the red component to remove the background image, because it is measured by using a red ray in the situation when the background is blue. The corresponding points are the center of gravity of the light source in the image. Fig.15 shows the result of the detection of corresponding points. In this figure, corresponding points have the same color.

Next, we evaluate the accuracy of computing corresponding points by simulation. Since the image of a light source is not a pixel, but has some area, an error in estimating the center of gravity occurs. We compare the corresponding points detected by this method with the theoretically computed ones, which are calculated by the equations described in Section 3.1.

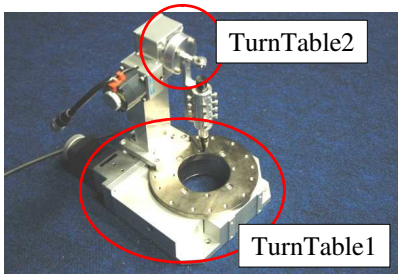

Figure 14: The calibration system

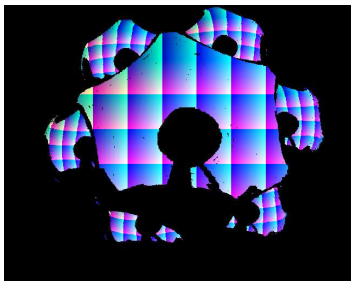

Figure 15: Measuring result of corresponding points

Table 1: Errors of corresponding points with/without the peripheral area of the mirrors

	With	Without
RMS[pixels]	0.814	0.696
SD[pixels]	0.300	0.190

We compared the results using the sensor that has a large mirror and 6 small mirrors. Their diameters are 50[mm] and 20[mm], the image size is 640×480[pixels] and the object is illuminated by a parallel light. We adjust the parameters of the simulation as a light source is projected with a 10×10[pixels^2] area in an image. We calculated the RMS and SD of the error as shown in Table 1. If we use the peripheral area of the mirrors, the error becomes large. Thus, we compare the results with/without the peripheral area of the mirrors. Since the errors are sufficiently small, our calibration method is validated as working without having to assume the shape of the sensor.

6.2 Detecting Objects by Simulation

In this section, we simulated a sensor for detecting an object around the sensor. The sensor has a large mirror and 6 small mirrors, and is shown in Fig.16. The diameters are 50[mm] and 20[mm], image size is 640×480[pixels].

The observed scene is shown Fig.18 and the input image is shown Fig.17. This scene consists of several poles with radii of 20[cm], which are set around the sensor at every

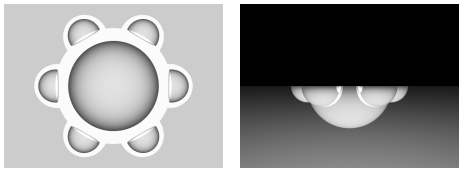

Vertical View Horizontal View

Figure 16: Configuration of compound spherical mirrors

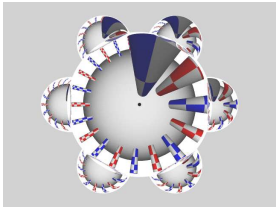

Figure 17: Input image used for simulation of detecting objects

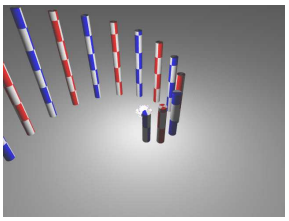

Figure 18: Scene used for simulation of detecting objects

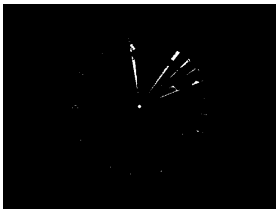

Figure 19: Result of detecting

50[cm] distance from the sensor. We detect the poles using the method described in Section 3. Fig.19 shows the detection result. The result shows that nearly a thirdlyof the poles can be detected. Then, the sensor can detect that an object exists within 150[cm]; however, it does not detect an object that exists over 200[cm].

6.3 Evaluation of Detectable Distance

In this section, we calculate the detectable distance of the sensor shown in Fig.20. Fig.21 shows the result of the detectable distance calculated by the method described in Section 5.2. The detectable distance is computed by the parallax between the center mirror and one of the side mirrors. Since the detectable distances are computed by 6 pairs of

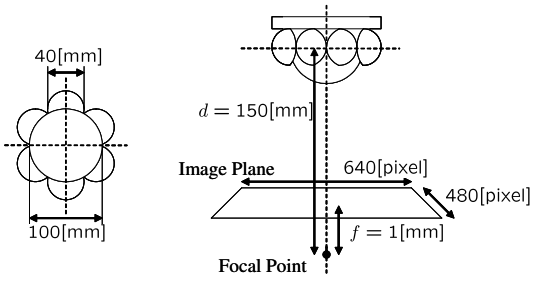

Figure 20: Parameter of the sensor that calculates detectable distance

mirrors, they are obtained by taking the maximum distance from those distances. As a result, the sensor can detect an object that exists within a distance of about 2.0[m]. This result matches the result of the above simulation.

Next, we consider that the sensor may be able to detect objects farther away, when using the parallax of the side mirrors. Thus, we calculate the corresponding points between the side mirrors, and calculate the detectable distances by the method described in Section 5.2. Fig.22 shows the result of the detectable distance. As a result, the result of the detectable distance is improved and the sensor can detect farther away objects.

However, it gets rise to a question about which parallax using is best to enhance the detectable distance. We compare detectable distance using adjacent side mirrors to that using side mirrors every second mirror. Fig.23 shows the result of the detectable distance by using adjacent side mirrors, and Fig.24 shows the result of the detectable distance by using side mirrors every second mirror. As a result, combinations of the side mirrors every second mirror contribute to detecting object.

Next, we analyze other parameter of detectable distance. Detectable distance is related resolution, mirror size, mirror design, and so on. In this paper, we analyzed relation of detectable distance, resolution and mirror size. We calculate relation, using the sensor shown in Fig.20 as base. Fig.25 shows the result of relation of the detectable distance and resolution. And, Fig.26 shows the result of relation of the detectable distance and mirror size.

There results show detectable distance is proportional to resolution and mirror size. Therefore, the sensor size can be made smaller without affecting the detectable distance by using high resolution camera and small mirror.

7 Conclusions

We have proposed a correspondenceless stereo system that consists of a single camera with multiple omnidirectional mirrors, which can detect approaching close objects without finding correspondences along epipolar lines. The system offers omnidirectional observation, portability, and real-time detection of near objects.

This paper described a method for calibrating a multiple omnidirectional mirror sensor through observing a point light source at an infinite range. For detecting near objects, the detection method needs a lookup table of points projected from of an object at an infinite range. When creating the table, the method requires for creating a model of the shape and location of the mirrors. Since it is difficult to make the model accurately, we proposed for calibrating a multiple omnidirectional mirror sensor through observing a point light source at an infinite range. It was sure the presented method was effective for not only compound spherical mirrors, but also mirrors of any shape. From the experiments, the calibration method was validated as working without having to assume the shape of the sensor.

Moreover, we analyzed detectable distances of the system with the mirrors of arbitrary shape. However, the system that consists of multiple mirrors make it difficult to theoretically calculate detectable distances. Thus, we also evaluated detectable distances at every pixel by analyzing in simulated experiments. As the result, it was proved that the detectable distance is enhanced by using a combination of various mirrors and that it was in proportion to the resolution of the image and the size of mirrors.

References

[1] R.Sagawa, N.Kurita, T.Echigo, Y.Yagi: "Compound Catadioptric Stereo Sensor for Omnidirectional Object Detection" *Proc.IEEE/RSJ International Conference on Intelligent Robots and Systems*, vol.2, pp.2612–2617, 2004.

[2] E.Mouaddib, R.Sagawa, T.Echigo, Y.Yagi: "Stereo Vision with a Single Camera and Multiple Mirrors" *Proc.IEEE International Conference on Robotics and Automation*, pp.812–817, 2005.

[3] H.Ishiguro, M.Yamamoto and S.Tsuji: "Omni-directional stereo" *IEEE Transactions on Pattern Analysis and Machine Intelligence*, 14,2,pp.257–262, 1992.

[4] S.Peleg and M.Ben-Ezra: "Stereo panorama with a single camera" *Proc.IEEE Conference on Computer Vision and Pattern Recognition*, Ft.Collins, Colorado, pp.395–401, 1999.

[5] J.Gluckman and S.Nayar: "Real-time omnidirectional and panoramic stereo" *Proc.of Image Understanding Workshop*, 1998.

[6] Y.Negishi, J.Miura, Y.Shirai: "Map Generation of a Mobile Robot by Integrating Omnidirectional Stereo and Laser Range Finder" *the Journal of the Robotics Society of Japan*, 21, 6, pp.690–696, 2003, in Japanese.

[7] A.Chaen, K.Yamazawa, N.Yokoya, and H.Takemura, "Omnidirectional stereo vision using hyperomni vision" *IEICE, Tech. Rep.*, pp.96–122, 1997, in Japanese.

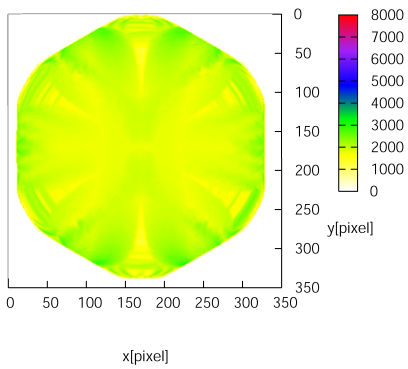

Figure 21: Detectable distance[mm]

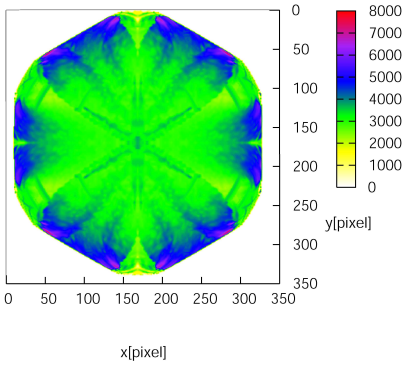

Figure 22: Detectable distance using parallax of side mirrors[mm]

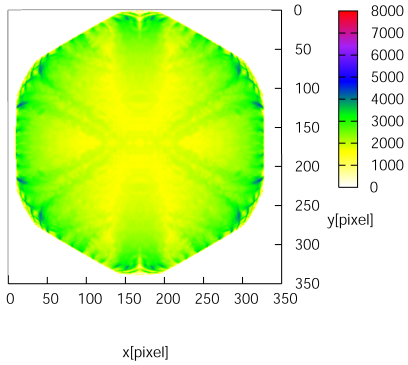

Figure 23: Detectable distance of using adjacent side mirrors[mm]

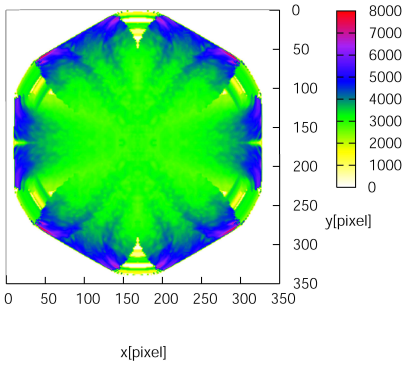

Figure 24: Detectable distance of using side mirrors every second mirror[mm]

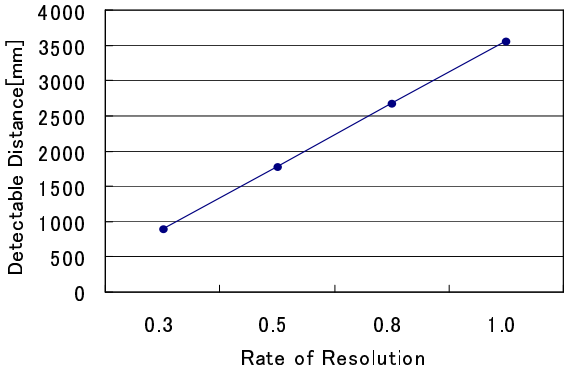

Figure 25: Relation of detectable distance and rate of resolution

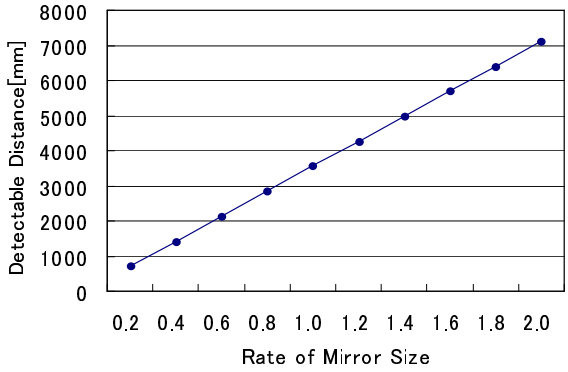

Figure 26: Relation of detectable distance and rate of mirror size